

## Short Communication

# The use of Raman spectroscopy to identify and grade prostatic adenocarcinoma *in vitro*

P Crow<sup>\*1</sup>, N Stone<sup>1</sup>, CA Kendall<sup>1</sup>, JS Uff<sup>1</sup>, JAM Farmer<sup>1</sup>, H Barr<sup>1</sup> and MPJ Wright<sup>2</sup>

<sup>1</sup>Cranfield Post-Graduate Medical School, Pullman Court, Gloucestershire Royal Hospital, Great Western Road, Gloucester, GL1 3NN, UK; <sup>2</sup>Bristol Royal Infirmary, Marlborough Street, Bristol, BS2 8HW, UK

Raman spectroscopy is an optical technique, which provides a measure of the molecular composition of tissue. Raman spectra were recorded *in vitro* from both benign and malignant prostate biopsies, and used to construct a diagnostic algorithm. The algorithm was able to correctly identify each pathological group studied with an overall accuracy of 89%. The technique shows promise as a method for objectively grading prostate cancer.

British Journal of Cancer (2003) 89, 106–108. doi:10.1038/sj.bjc.6601059 www.bjcancer.com  
© 2003 Cancer Research UK

**Keywords:** prostate cancer; benign prostatic hypertrophy; Raman spectroscopy; Gleason score

Raman spectroscopy is an optical technique that utilises molecular-specific, inelastic scattering of light photons to interrogate biological tissues (Mahadevan-Jansen *et al*, 1998). When tissue is illuminated with laser light, photons interact with intramolecular bonds present within the tissue. When occurs, the photon donates energy to or receives energy from the bond, producing a change in the bond's vibrational state. When it subsequently exits the tissue, the photon has an altered energy level and, therefore, has a different wavelength compared to the original laser light. This change in the photon's energy is known as the 'Raman shift' and is measured in wavenumbers. Photons interacting with different biochemical bonds within the tissue, undergo different Raman shifts, which taken together, form the 'Raman spectrum'. The Raman spectrum is a plot of intensity against Raman shift, in wavenumbers. As the Raman Shift is inversely proportional to the change in the photons' wavelength, wavenumbers are expressed in units of  $\text{cm}^{-1}$ . The Raman spectrum is a direct function of the molecular composition of the tissue and can therefore give a truly objective picture of the pathology. This is in contrast to Gleason grading, which is subjective and associated with considerable interobserver variation in reporting (Allsbrook *et al*, 2001a, b). A previous study has confirmed that it is possible to record good-quality Raman spectra from prostatic tissue (Crow *et al*, 2002); this study evaluates the ability of Raman spectroscopy to differentiate between different prostatic pathologies *in vitro*.

## MATERIALS AND METHODS

Ethical approval was obtained to take an extra core at prostate biopsy procedures. These biopsies were snap frozen in liquid nitrogen and transferred to a  $-80^{\circ}\text{C}$  freezer for storage. A frozen section was taken from each biopsy and processed for standard

histological examination, and the remainder of the biopsy was retained at  $-80^{\circ}\text{C}$ . The sections were examined by a Consultant Uro-Pathologist and histological diagnosis was made. Those sections containing prostate adenocarcinoma were then examined by a second Consultant Pathologist. In order to minimise the effects of interobserver variation in Gleason scoring, biopsies were only included in the study where an agreement on the Gleason score (GS) was reached between the two pathologists. The position of the prostate cancer within each section was carefully mapped so that the region could subsequently be accurately targeted on the Raman system. Biopsies were classified as benign prostatic hyperplasia (BPH) or adenocarcinoma, with the adenocarcinoma group further split into three groups depending on Gleason score (GS less than seven, GS equal to seven and GS greater than seven).

The remainder of each prostate biopsy, from which the section had been taken, was thawed in preparation for scanning on an optimised Raman system (Renishaw System 1000). The system employs a diode laser, producing 350 mW of near-infrared light at 832 nm. The laser was accurately targeted onto the tissue sample via an ultralong working distance times 80 microscope objective. This produces a laser spot of approximately 30 square microns, which penetrates the tissue up to a depth of 100  $\mu\text{m}$ . The information held within each Raman spectrum, therefore, relates to a cluster of around 30 cells. Using the histological map provided by the pathologist, the laser spot was targeted precisely onto an area of known pathology within each sample. The laser spot was then moved to random locations within this known area, to allow up to 20 spectra to be recorded from each sample. Each Raman spectrum was recorded on the spectrometer using an acquisition period of 20 s. A total of 450 spectra were measured from biopsies taken from 27 different patients, 14 with BPH and 13 with adenocarcinoma.

The spectral data were loaded onto the Matlab platform (Mathworks Inc., Natick, Massachusetts), which, in conjunction with the PLS Toolbox (eigenvector, Manson, Washington), was used to perform the principal component fed, linear discriminant analysis required to construct a diagnostic algorithm. The accuracy

\*Correspondence: Mr P Crow; E-mail: paul\_crow@hotmail.com

Received 17 December 2002; revised 8 April 2003; accepted 10 April 2003

of the algorithm, in correctly predicting the histological diagnosis for each spectrum, was tested using 'leave one spectrum out' crossvalidation. This ensured that the data from the spectrum, which was having its diagnosis predicted by the algorithm, had not been used in constructing the algorithm being tested. A qualitative analysis was also undertaken by comparing the mean of the spectra recorded from BPH with the mean of the spectra recorded from all prostate cancers.

## RESULTS

Figure 1 shows mean, spectra for each pathological group studied. In the interests of clarity, the spectra have been arranged so that they are equally spaced with respect to the intensity axis. Figure 2 illustrates the prediction power of the algorithm, with the algorithm-predicted diagnosis plotted against the confirmed histological diagnosis.

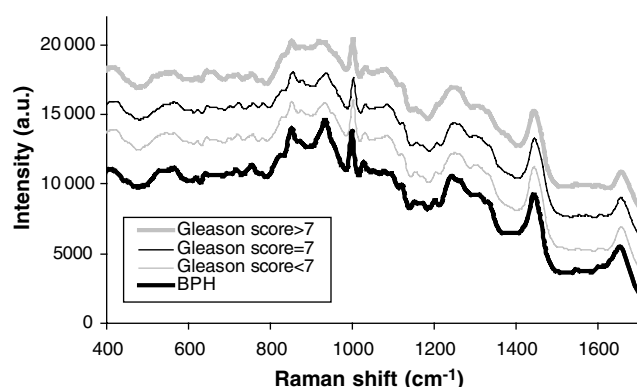


**Figure 1** The Mean Raman spectra for each pathological group studied.

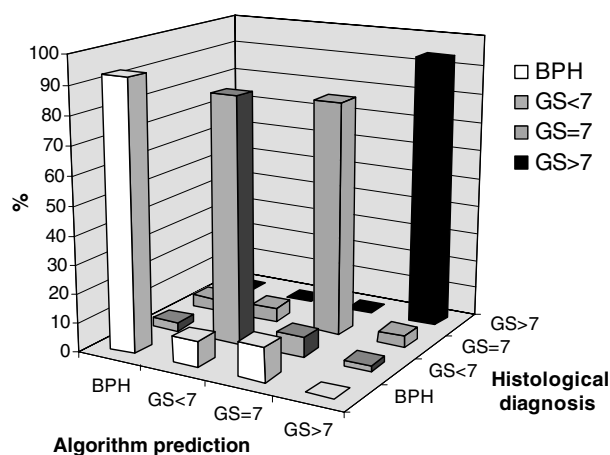


**Figure 2** Bar chart and grid demonstrating the prediction power of the diagnostic algorithm.

correspond to the correct prediction of histological diagnosis, with the other small columns representing misdiagnoses by the algorithm. The rows of Table 1 show the confirmed histological diagnosis for each spectrum measured. The table columns show the diagnosis predicted by the algorithm for each spectrum measured. By reading across each row, the number of correct and incorrect algorithm predictions, for each histological diagnosis, can be viewed. Table 2 shows how the algorithm's predictive accuracy translates to sensitivity and specificity for each pathological group studied.

**Table 1** Confirmed histological diagnosis against the diagnosis predicted by the algorithm

Prediction	Histological diagnosis	Algorithm			
		BPH	GS <7	GS = 7	GS >7
	BPH	192	6	9	0
	GS <7	11	99	6	0
	GS =7	10	6	70	0
	GS >7	0	1	2	44

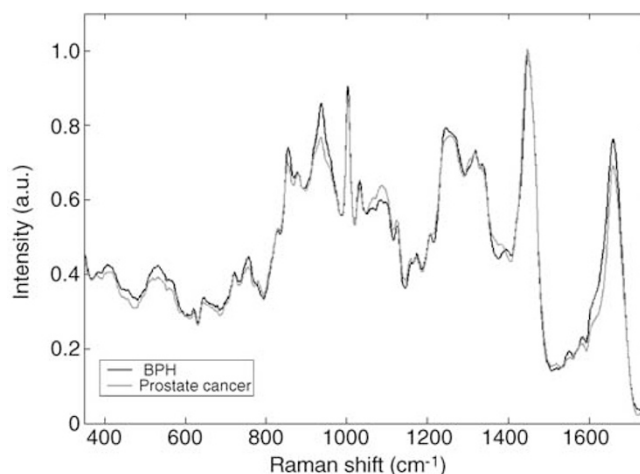


**Figure 3** The mean Raman spectra recorded from BPH and all prostate cancers studied.

Figure 3 shows the mean spectra recorded from BPH and all prostate cancers studied. Where visual differences in the peak heights of the two spectra were noted, the relevant literature was consulted for information as to the nature of these peaks (Hartman *et al*, 1973; Manoharan *et al*, 1995; Boustany *et al*, 1996; Mahadevan-Jansen, 1996; Manfait *et al*, 2000; Stone *et al*, 2002). Although the biochemical designations of many peaks remain uncertain, the differences between the two mean spectra suggest that prostate cancer has increased levels of nucleic acids and reduced levels of glycogen, when compared to BPH.

## DISCUSSION

This study shows that Raman spectroscopy can be used to accurately identify BPH and three different grades of prostatic adenocarcinoma *in vitro*. Snap-frozen samples were used in order to reproduce *in vivo* conditions as closely as possible, however, work carried out by our group on other tissues has confirmed that the technique can achieve similar results with formalin-fixed specimens (Stone, 2001). The technique therefore shows promise as a pathology tool providing a rapid, objective method for diagnosing and grading prostate cancer. Work is ongoing to increase the sample size of the study and also to determine whether the technique is able to provide prognostic information for individual patients with prostate cancer. Potential *in vivo* applications include use, via a needle probe, to guide prostatic biopsy and allow intraoperative assessment of tumour resection margins.

The qualitative findings of reduced glycogen content and increased nucleic acid content in malignant, compared to benign pathologies, fit in with the findings of previous studies of the larynx (Stone *et al*, 2000), colon (Feld *et al*, 1995), oesophagus

**Table 2** Sensitivity and specificity achieved by the diagnostic algorithm for each pathological group

	BPH	Gleason score <7	Gleason score =7	Gleason score >7
Total no. of spectra/ (total no. of patients)	207 (14)	116 (6)	86 (4)	47 (3)
Sensitivity	93%	85%	81%	94%
Specificity	92%	96%	96%	100%

(Bakker Schut *et al*, 1997) and cervix (Mahadevan-Jansen *et al*, 1998). These findings provide an insight into the type of molecular differences, which allow the technique to differentiate between the different pathologies. The use of multivariate spectral analysis ensures that the diagnostic algorithm is constructed using all the molecular information available from the Raman spectra. Retrieving quantitative biochemical information from the Raman spectra of prostatic tissue, however, currently remains a prospect for the future.

## REFERENCES

- Allsbrook Jr WC, Mangold KA, Allsbrook WC, Johnson MH, Lane RB, Lane CG, Amin MB, Bostwick DG, Humphrey PA, Jones EC, Reuter VE, Sakr W, Sesterhenn IA, Troncoso P, Wheeler TM, Epstein JI (2001a) Interobserver reproducibility of Gleason grading of prostatic carcinoma: urologic pathologists. *Hum Pathol* 32(1): 74–80
- Allsbrook Jr WC, Mangold KA, Johnson MH, Lane RB, Lane CG, Epstein JI (2001b) Interobserver reproducibility of Gleason grading of prostatic carcinoma: general pathologist. *Hum Pathol* 32(1): 81–88
- Bakker Schut TC, Van Dekken H, Tilanus HW, Bruining HA, Puppels GJ (1997) NIR Raman spectroscopy of healthy and diseased oesophagus. In *Spectroscopy of Biological Molecules: Modern Trends*, Carmona P, Navarro R, Hernanz A (eds) pp 455–456. Dordrecht: Kluwer Academic Publishers
- Boustany NN, Manoharan R, Dasari RR, Feld MS (1996) Analysis of normal and diseased colon mucosa using ultraviolet resonance Raman spectroscopy. *Proc SPIE: Adv Laser Light Spectros Diagnose Cancer Diseases III: Opt Biopsy* 2679: 66–70
- Crow P, Kendall C, Ritchie A, Wright M, Stone N (2002) Evaluation of Raman spectroscopy to provide a real time, optical method for discrimination between normal and abnormal tissue in the prostate. *Eur Urol* 1(Suppl 1): 80
- Feld MS, Manoharan R, Salenius J, Orenstein-Carndona J, Romer TJ, Brennan JF, Dasari R, Want Y (1995) Detection and characterization of human tissue lesions with near-infrared Raman spectroscopy. *Proc. SPIE: Adv Fluorescence Sensing Technol II* 2388: 99–104

## ACKNOWLEDGEMENTS

We thank Mr HW Gilbert, Mr ASW Ritchie and Mr DJ Jones for their assistance in providing the tissue for the study, along with Jackie and Christine who prepared the histological sections. We are also grateful to Ms J Reyes-Goddard and Mr RA Persad for their continued support in this research.

- Hartman KA, Clayton NW, Thomas Jr GJ (1973) Studies of virus structure by Raman spectroscopy. *Biochem Biophys Res* 50: 942
- Mahadevan-Jansen A, Richards-Kortum R (1996) Raman spectroscopy for the detection of cancers and precancers. *J Biomed Opt*, 1: 31–70
- Mahadevan-Jansen A, Mitchell MF, Ramanujam N, Malpica A, Thomsen S, Utzinger U, Richards-Kortum R (1998) Near-infrared Raman spectroscopy for *in vitro* detection of cervical precancers. *Photochem Photobiol* 68: 123–132
- Manfait M, Lamaze P, Lamfarraj H, Pluot M, Sockalingum GD (2000) Diagnosis and prognosis of tissue pathologies by Raman microspectroscopy: an application to human thyroid tumours. *Proc SPIE: Biomed Spectros: Vib Spectros Novel Tech* 3918: 153–160
- Manoharan R, Wang Y, Dasari RR, Singer SS, Rava RP, Feld MS (1995) Ultraviolet resonance Raman spectroscopy for detection of colon cancer. *Laser Life Sci* 6(4): 217–227
- Stone N (2001) Raman spectroscopy of biological tissue for application in optical diagnosis of malignancy. PhD Thesis, *Cranfield University*, pp 137–148
- Stone N, Stavroulaki P, Kendall C, Birchall M, Barr H (2000) Raman spectroscopy for early detection of laryngeal malignancy: preliminary results. *Laryngoscope* 110: 1756–1763
- Stone N, Stavroulaki, Kendall C, Shepherd N, Crow P, Barr H (2002) Near-infrared Raman spectroscopy for the classification of epithelial precancers and cancers. *J Raman Spectrosc* 33: 564–573